Evaluation of cloud effects on air temperature estimation using MODIS LST based on ground measurements over the Tibetan Plateau

Hongbo Zhang[1, 2], Fan Zhang[1, 2], Guoqing Zhang[1, 2], Xiaobo He[3], Lide Tian[1, 2]

[1] Key Laboratory of Tibetan Environment Changes and Land Surface Processes, Institute of Tibetan Plateau Research, Chinese Academy of Sciences, Beijing, China

[2] CAS Center for Excellence in Tibetan Plateau Earth Sciences, Beijing, China

[3] Cold and Arid Regions Environmental and Engineering Research Institute, Chinese Academy of Sciences, Lanzhou, China

Correspondence to: Hongbo Zhang, Tel.: +86-10-84097030; fax: +86-10-84097079.

E-mail address: zhanghongbo@itpcas.ac.cn

Abstract

Moderate Resolution Imaging Spectroradiometer (MODIS) daytime and nighttime land surface temperature (LST) data are often used as proxies for estimating daily maximum (T_{max}) and minimum (T_{min}) air temperatures, especially for remote mountainous areas due to the sparseness of ground measurements, However, the Tibetan Plateau (TP) has a high daily cloud cover fraction (>45%), which may affect the air temperature (T_{air}) estimation accuracy. This study comprehensively analyzes the effects of clouds on T_{air} estimation based on MODIS LST using detailed half-hourly ground measurements and daily meteorological station observations collected from the TP. It is shown that erroneous rates of MODIS nighttime cloud detection are obviously higher than those achieved in daytime. Large errors in MODIS nighttime LST data were found to be introduced by undetected clouds and thus reduce the T_{min} estimation accuracy. However, for T_{max} estimation, clouds are mainly found to reduce the estimation accuracy by affecting the essential relationship between T_{max} and daytime LST. The obviously larger errors of T_{max} estimation than those of T_{min} could be attributed to larger MODIS daytime LST errors resulting from higher degrees of LST heterogeneity within MODIS pixel than those of nighttime LST. Constraining MODIS observations to non-cloudy observations can efficiently screen data samples for accurate T_{min} estimation using MODIS nighttime LST. As a result, the present study reveals the effects of clouds on T_{max} and T_{min} estimation through MODIS daytime and nighttime LST, respective, so as to help improve the T_{air} estimation accuracy and alleviate the severe air temperature data sparseness issues over the TP.

Keywords: cloud effects, MODIS LST, air temperature estimation, Tibetan Plateau

1 Introduction

Air temperature is a key variable used to describe environmental conditions. However, temperature observations are typically sparse in remote mountainous areas (Lin et al., 2016). Remotely sensed land surface temperatures (LST) can serve as an efficient proxy for air temperature estimation in such areas. Superior to limited ground measurements, remote sensing can provide more spatiotemporal information. Several studies have estimated air temperatures using Moderate Resolution Imaging Spectroradiometer (MODIS) land surface temperature products for Europe (Benali et al., 2012; Kilibarda et al., 2014), Canada (Xu et al., 2014), USA (Oyler et al., 2015; Parmentier et al., 2015; Oyler et al., 2016), Africa (Vancutsem et al., 2010; Lin et al., 2012), western Asia (Emamifar et al., 2013) and the Tibetan Plateau (TP) (Fu et al., 2011; Zhu et al., 2013).

Due to its high altitudes, the TP and surroundings include the largest cryosphere area outside the Arctic and Antarctic regions and outside Greenland, and it is considered to be among the areas that are most sensitive to climate change. However, most meteorological stations in the TP are located in low-altitude (< 4800 m) and eastern regions (Fig. 1). There are almost no stations in the vast western area or at the elevations above 5000 m. In particular, for glacier covered areas, temperature observations are extremely scarce (Wu et al., 2015). Remotely sensed LSTs can greatly help alleviate the problems associated with scarce temperature observations available for the TP.

Despite the advantages of high spatial and temporal accessibility to large-scale areas, remote sensing data present some limitations, among which cloud contamination issues may be the most important. For applications of MODIS LST, clouds can affect the T_{air} estimation in at least two ways: erroneous cloud identification can reduce the accuracy of MODIS LST values, and the presence of clouds can affect the relationship between LST and T_{air} and can further affect the accuracy of T_{air} estimations.

The presence of clouds can greatly decrease the amount of data available in the satellite images. Moreover, the existing cloud detection algorithms cannot identify all the cloudy pixels, and a considerable percentage of undetected cloudy pixels exists in MODIS LST products (reported at roughly 15%) (Ackerman et al., 2008). It has been shown through some validation studies that extremely large differences (>10 K) between MODIS LST and ground measurements occasionally

occur, even for homogeneous surfaces. In these cases, the cloud top temperatures can be taken as the LST values (Langer et al., 2010; Westermann et al., 2011). More recently, up to 40% of ground measured cloudy samples have been labeled unidentified according to field observations, thus producing rather large MODIS LST errors, as reported for Svalbard (Østby et al., 2014). Such errors can disturb the true relationship between LST and air temperatures (T_{air}). MODIS daytime LST has been found to be affected by unidentified cloudy pixels, causing such pixels to severely degrade LST-T_{air} relationships (Williamson et al., 2013). Because the daytime cloud algorithm is expected to present more confidence than that for nighttime (Ackerman et al., 1998), using the nighttime LST for air temperature estimation may be influenced more by undetected clouds. For the TP, cloud contamination also constitutes a major problem, generating a mean daily cloud cover fraction of > 45% (Yu et al., 2016). Thus, the effects of clouds are particularly essential for T_{air} estimation in the TP.

In addition to the effects of undetected cloudy pixels, clouds are expected to play a key role in the relationship between LST and T_{air} due to its cooling effects during the day and warming effects at night (Dai et al., 1999). During the day, clouds can decrease land surface warming rates by blocking solar radiation, and at night, clouds can reflect surface long wave radiation and decrease heat losses from the land surface producing higher ground temperatures than those detected on clear days. For example, the difference between observed daytime LST and T_{air} under cloudy conditions is much lower (an average of ~3.7 °C) than that observed under clear conditions (Gallo et al., 2011). Therefore, questions regarding whether and how clouds can affect relationships of T_{max}-Daytime LST and T_{min}-Nighttime LST have been posed. Previous T_{air} estimation based on MODIS LST are presumably valid for clear conditions (Shen and Leptoukh, 2011; Oyler et al., 2015). However, satellite observed LSTs (in night or day) are instantaneous and may have a time lag between the overpass time and the time when T_{air} reaches its minimum or maximum. Daily cloudiness conditions may affect the warming (during the day) or cooling (at night) rates and can further alter the relationship between T_{air} and LST.

Previous studies have mainly focused on two types of daily T_{air} estimations: daily maximum (T_{max}) and minimum (T_{min}) air temperatures (Benali et al., 2012; Xu et al., 2014; Good, 2015). In addition, daytime and nighttime LST have been used as predictors for T_{max} and T_{min} estimations, respectively, due to their different overpass times (Vancutsem et al., 2010; Lin et al., 2012; Oyler

et al., 2016). Recent studies have interestingly found that the estimation accuracy of T_{max} based on daytime LST is clearly lower than that of T_{min} based on nighttime LST (Zhang et al., 2011; Benali et al., 2012; Oyler et al., 2016), and nighttime LST has an even higher correlation with T_{max} than daytime LST (Zhang et al., 2011; Zeng et al., 2015). Benali et al. (2012) hypothesized that the presence of cloud cover may decrease daytime warming levels, resulting in incorrect modeling and negative effects of cloud cover on estimation accuracies. Oyler et al. (2016) instead attributed this to the large microscale variability differences between daytime and nighttime LST.

Due to the scarcity of detailed cloud observations available, few studies have focused on the potentially important effects of clouds on estimations of T_{air} using remotely sensed LST. This study explores the effects of clouds on T_{air} estimation using MODIS LST based on detailed half-hourly ground measurements and the daily China Meteorological Administration (CMA) station observations. For the TP, sufficiently detailed observations are extremely rare and related studies have not been conducted before. Three automatic weather stations (AWS) with half-hourly averaged observations are examined in this study, including one valuable site positioned on the glacier. To make our study more representative, data drawn from 92 CMA stations that include daily T_{max} and T_{min} observations are also used for cloud effect tests.

2 Data

2.1 Ground measurements

In this study, detailed observations from three AWSs on the TP were obtained (Fig. 1). The Ngari station is located in the western area of the TP at an elevation of 4270 m. Desert grassland constitutes the main form of land cover here. The Qinghai station is located in the northeastern TP at an elevation of 3250 m and is dominated by alpine meadow. The Xiao Dongkemadi station is located in the interior TP at an elevation of 5621 m on the Xiao Dongkemadi glacier (Fig. 1). The general features of the three AWSs are listed in Table 1. In addition, daily T_{max} and T_{min} observations measured at 2 m above the ground surface from 92 CMA stations over the TP are also used for assistant analysis. Data drawn from these CMA stations are for 2007 to 2010.

All three AWSs provide half-hourly averaged ingoing and outgoing longwave radiation, and air temperature data. Through controlling the data quality did by the data provider, obvious outliers have been removed for all three AWSs. These radiation data were measured using a widely used CNR1 net radiometer, at an uncertainty level of ±10% for daily totals by the manufacture. Air

temperatures were collected using an HMP45C sensor with expected accuracies of ±0.2–0.5 °C depending on the temperature ranges involved. Detailed measurement specifications are listed in Table 1. However, only the Xiao Dongkemadi station provides the directly measured LST values which were obtained through an Apogee Precision Infrared Thermocouple Sensor (IRTS-P) with an accuracy of 0.3 K over the glacier surface (Huintjes et al., 2015). The LSTs of the Qinghai and Ngari stations were derived based on the Stefan–Boltzmann law and the thermal radiative transfer theory:

$$L_u = \sigma T_b^4 = (1-\varepsilon)L_d + \varepsilon\sigma T_s^4 \qquad (1)$$

where L_u and L_d are the upwelling and downwelling longwave radiation, respectively, σ is the Stefan–Boltzmann constant (5.670367×10^{-8} Wm^{-2} K^{-4}), ε is land surface emissivity, T_b is the brightness temperature, T_s is the land surface temperature. The calculated LSTs were taken as ground measurements of LST as Wang et al. (2008).

In this study, emissivity values were assigned empirically due to a lack of measurements. Emissivity values for the Qinghai and Ngari stations were set to 0.987 (alpine meadow) and 0.975 (desert grassland), respectively, according to Wang et al. (2008). To partly quantify the effects of emissivity value uncertainty, simple sensitivity tests were conducted. A 0.001 change in emissivity is on average found to result in the LST change of 0.015 K and 0.020 K for stations Qinghai and Ngari, respectively.

2.2 MODIS Land Surface Temperatures

Daily 1-km LST products of MODIS level 3 collection 5 are used in this study including the data from the Terra (MOD11A1) and Aqua (MYD11A1) satellites. Both Terra and Aqua generate two daily observations, including one for the daytime and one for nighttime. The two overpass times for Aqua are approximately 1:30 and 13:30 local time. For Terra, these times are approximately 10:30 and 22:30. Accurate view times can be derived from the product. The MODIS LST used here is retrieved using the generalized Split-window algorithm (Wan and Dozier, 1996). Accuracies are reported to range within 1 K, but the uncertainties and errors of emissivity used in the MODIS LST product can be significant, which produces major errors (Wan et al., 2002). Each grid of the MODIS LST product includes a quality control (QC) flag that ranges from 0 to 3 indicating the average errors of <1 K, 1−2 K, 2−3 K and >3 K. Records with a QC flag of 3 were

omitted in this study.

The MODIS observations are instantaneous, whereas the ground measurements used are half-hourly averaged. To make them comparable, the timing of ground observations recorded on Beijing time was converted to local solar time. Then, half-hourly observations that are within 15 minutes of the view times of MODIS record times were selected.

3 Methods

The procedure for analyzing cloud effects step by step are outlined in Fig. 2, and described in detail as followed.

3.1 Cloud index estimations

Cloud observations are usually only available from non-automatic weather stations and are difficult to record. In this study, an efficient method was employed to estimate cloudiness based on downwelling longwave radiation (L_d) records and air temperatures, which have been widely used in other studies (Giesen et al., 2008; Yang et al., 2011; Østby et al., 2014). This theory is mainly based on the principle that under cloudy conditions, a longwave radiation balance exists between cloud base and near surface (Giesen et al., 2008; Østby et al., 2014). Under overcast conditions, both the cloud base and near surface radiate at similar temperatures and L_d reaches its max. However, L_d should be much lower under clear conditions than under overcast conditions under the same temperature. In such a case, L_d reaches its minimum. Thus, a max L_d can be reversed using the Stefan–Boltzmann law under a given air temperature, and the min L_d can be regressed using the polynomial fit of the lower 5th percentile of the L_d observations for each specified temperature interval (1 K here) (Østby et al., 2014). When L_d is assumed to linearly increase from clear to overcast conditions at a given temperature, then a “cloud index” (CI) indicating the cloudiness can be achieved (CI = 0 and 1 for clear and overcast skies respectively) (Giesen et al., 2008; Yang et al., 2011; Østby et al., 2014). For example, for an observed downwelling longwave radiation as L_i at the temperature T_i, if the L_{max} and L_{min} are the maximum and minimum L_d under that temperature (T_i) respectively, then the CI is determined as $(L_i - L_{min}) / (L_{max} - L_{min})$. Rather than the visually observed percentage of cloud cover in the sky, the CI used here represents the optical thickness of clouds (Van Den Broeke et al., 2006).

3.2 Testing cloud effects on the accuracies of MODIS LST

Undetected clouds may exist in the MODIS LST data as a result of erroneous cloud identification. An evaluation of the number of undetected clouds present was firstly conducted. As considerable errors can be introduced by undetected clouds, the effects of clouds on MODIS LST accuracies were evaluated by comparing validation (MODIS vs. observed LST) results derived before and after removing the undetected cloudy records. In this study, the records with CI > 0.5 are considered to be under "mostly cloudy" conditions. For a given MODIS observation, it is regarded as undetected cloud if its corresponding CI > 0.5.

In this study, all four MODIS observations derived from the Terra and Aqua satellites were validated to identify and explain the effects of clouds on T_{air} estimations. It should be noted that the effects of undetected clouds may come from or be mixed with the effects of residual/thin clouds (Platnick et al., 2003), fogs (Østby et al., 2014) and some thick aerosol layers (Huang et al., 2014) existing in the MODIS pixel, which may impose errors on the MODIS LST product to varying degrees. Even though these effects are hard to distinguish in detail, undetected clouds are generally considered to have strong negative effects on the accuracies of MODIS LST (Williamson et al., 2013; Østby et al., 2014; Shamir and Georgakakos, 2014).

3.3 T_{air} estimation

Various statistical methods have been used for T_{air} estimation using MODIS LST, including neural network (Jang et al., 2004), random forests (Xu et al., 2014), M5 model tree (Emamifar et al., 2013) and the simple linear regression (Zhang et al., 2011; Benali et al., 2012; Lin et al., 2012). Comparisons among the performances of six types of statistical models with different levels of complexity for T_{air} estimation indicate that though there truly exist some cases where advanced statistical models clearly outperform the simple linear regression model, the absolute differences of accuracies produced by different models are generally not big, especially for cases using MODIS nighttime LST (Zhang et al., *in press*). Compared with the complex models such as neural network and random forests which introduce uncertainties owing to their much larger number of parameters, the linear regression model has the advantage of being easy to interpret and is most commonly used in previous studies (Zhang et al., 2011; Benali et al., 2012; Lin et al., 2012). In addition, an individual linear fit is built for each AWS or CMA station to make the relationship

between T_{air} and LST as locally accurate as possible and thus, variables indicating spatial coordinates (longitudes and latitudes) and land cover (e.g. NDVI) are not used. Therefore, the linear regression model using LST as the single independent variable is chosen as the T_{air} estimating method in this study.

3.4 Testing cloud effects by the observed LST

Large MODIS LST errors may exist due to undetected clouds, and cloud effects are first tested using the ground measured LST. In this way, we can explore the direct effects of clouds on T_{air} estimation using LST. The tests are conducted by constraining cloudiness conditions. Target T_{air} values in most studies are daily (max, mean or min) values, but instantaneous cloudiness is meaningless. In this study, the daily mean CI value is used as a cloudiness indicator. To ensure a sufficient number of samples, 9 types of conditions with daily mean CI values $\leq$ 0.2, 0.3, …, 0.9 and 1.0 are employed, indicating that the cloudiness constraints vary from highly clear conditions (daily mean CI $\leq$ 0.2) to fully mixed conditions, with many highly cloudy days included (daily mean CI $\leq$ 1.0). For each condition, T_{max} and T_{min} are regressed using daytime (13:30, Aqua) and nighttime (22:30, Terra) observed LST through a simple linear regression, and estimation accuracies are computed. The root-mean-square error (RMSE) and mean absolute error (MAE) are used as the accuracy measurements. Cloud effects are evaluated based on the variation of the estimation accuracies under different cloudiness conditions. Comparisons of T_{max} and T_{min} estimations can reveal further implications of cloud effects.

3.5 Determining cloud effects through comparisons using MODIS and the observed LST

Once the effects of clouds on T_{air} estimations using observed LST are confirmed, cloud effects on T_{air} estimation using MODIS LST can be explored more directly. Apart from affecting the relationship between T_{air} and MODIS LST, clouds can degrade the MODIS LST accuracy and further reduce estimation accuracies. Such effects, when they are present, can be explored by comparing changes in estimation accuracy levels between observed LST and MODIS LST. Here, T_{air} (T_{min} and T_{max}) estimations for 9 kinds of CI conditions are conducted using MODIS LST and observed LST (at the corresponding MODIS time), respectively. The results are analyzed based on comparisons.

3.6 Exploring cloud effects based on observations from meteorological stations

In practice, only daily observations can be easily obtained from meteorological stations, and cloudiness observations are usually not provided. In this study, only daily T_{max} and T_{min} data are obtained from the 92 CMA stations. Nonetheless, daily cloudiness levels can be partly evaluated from four MODIS observations for each day (two from Terra and two from Aqua). Then, comparisons of T_{air} estimation for two distinct cloudiness conditions are drawn.

Two conditions ("cloudy day" and "non-cloudy day") are defined based on four instantaneous MODIS observations for each day for both the T_{max} and T_{min} estimation using Aqua daytime LST and Terra nighttime LST, respectively. For "non-cloudy day" conditions, all four MODIS cloudiness observations are constrained as non-cloudy. For the "cloudy day" condition of the T_{max} estimation, Aqua daytime observations are constrained as non-cloudy to obtain the available LST, and Terra daytime observations are constrained as cloudy to make cloud effects as strong as possible. However, the Aqua night and Terra night observations are not constrained to obtain sufficient samples. For the "cloudy day" condition of the T_{min} estimation, the Terra nighttime observations are constrained as non-cloudy to obtain the available LST, whereas the Aqua nighttime observations are not constrained to obtain sufficient samples. Both Aqua daytime and Terra daytime observations are constrained as cloudy to make the cloud effects as strong as possible. T_{max} and T_{min} estimation accuracies are then compared under "cloudy day" and "non-cloudy day" conditions.

4 Result

4.1 Cloud index estimation and the undetected clouds of MODIS

Figure 3 shows that the maximum and minimum L_d curves effectively frame L_d variation for each air temperature. The CI values of all of the observations are then computed.

For each of the four overpass times of MODIS LST, a rate of undetected cloudy records can be determined using CI values (Table 2). The ratio of undetected cloudy records ranges from 3% to 50% with a fully averaged ratio of 15%. This agrees well with the reported value of ~15%, which was computed based on a consistency comparison between MODIS and Lidar (Ackerman et al., 2008).

4.2 MODIS LST validation under different cloud conditions

The accuracy of MDOIS LST can be affected by undetected cloudy pixels (Westermann et al., 2012; Shamir and Georgakakos, 2014). Figure 4 shows that after removing cloudy cases, the validation accuracies of all three sites present obviously lower MAE values and a better fit line slope. Improvements in accuracy for 6 (2 pass times × 3 stations) nighttime cases range from 0.1 to 0.9 °C. However, no significant accuracy improvements were found after removing cloudy cases for daytime MODIS LST (Fig. 5). Only slightly better or comparative MAEs (≤0.1 °C) were obtained.

This indicates that the accuracy of MODIS nighttime LST is more negatively affected by undetected clouds than that for the daytime. The relatively weak influences of undetected clouds on daytime LST is mainly due to obviously lower erroneous rates of cloud detection compared to those of nighttime LST. Erroneous rates of MODIS nighttime cloud detection are clearly larger than those for the daytime, though not in the case of the Terra LST observed for Ngari. This can be largely attributed to differences in cloud detection methods used for the daytime and nighttime. The cloud detection algorithm of MODIS is considered to present more confidence for the daytime than for the nighttime due to the absence of reflected solar radiation during nighttime (Ackerman et al., 1998). This finding is consistent with previous studies showing that more than 40% of the observed cloudy days are identified as clear days by MODIS at polar summer nighttime (Østby et al., 2014).

4.3 The effects of clouds on T_{air} estimation based on ground observed LST

Figure 6 shows the accuracy of T_{air} estimations based on ground observed LST under different cloudiness conditions across the three sites. For T_{max}, estimation errors including RMSE and MAE continually increased as the cloudiness condition constraints eased. The increase in RMSE/MAE values for clear conditions (daily mean CI ≤ 0.2) compared with totally mixed conditions (daily mean CI ≤1) was 1.3 °C/1.0 °C, 0.8 °C/0.8 °C and 1.6 °C/1.6 °C for the Ngari, Xiao Dongkemadi and Qinghai stations, respectively. In contrast, for T_{min}, accuracy variation is consistently mild across the three sites, presenting RMSE/MAE changes of 0.1 °C/0.0 °C, 0.1 °C/0.0 °C, and 0.7 °C/0.6 °C for the Ngari, Xiao Dongkemadi and Qinghai stations,

311 respectively. It should be noted that when the “cloudiness condition” exceeds 0.6 (x > 0.6), the
312 sample number no longer varies and due to the limited number of samples, the variation of T_{max}
313 and T_{min} estimating accuracy is rather flat.
314 As expected for cases based on ground observed LST, the T_{max} estimation is significantly affected
315 by cloud conditions, but clouds have a limited effect on the T_{min} estimation compared to T_{max}. This
316 interesting finding can be explained by mechanisms through which clouds affect nighttime and
317 daytime surface temperatures. In the daytime, LST is significantly influenced by solar heating.
318 The presence of clouds can screen out solar radiation and cool the surface. Much larger
319 differences between LST and T_{air} have been observed under cloudy days than under clear
320 conditions (Gallo et al., 2011). At night, the surface can also present warming effects from clouds
321 due to reflected infrared longwave radiation. However, such effects are not typically significant
322 because the net effect of clouds on surface downward longwave radiation is much less pronounced
323 than nighttime solar cooling effects in most cases, as indicated by Dai et al. (1999).
324
325 **4.4 The effects of clouds on T_{air} estimation based on MODIS LST**
326 Figure 7 compares cloud effects on T_{min} and T_{max} estimations using MODIS and observed LST.
327 First, despite rather mild effects of cloud conditions on T_{min} estimation based on ground observed
328 LST, those based on MODIS LST are clearly much more significant. For cases based on MODIS
329 LST, increases in RMSE between clear (daily mean CI $\leqslant$ 0.2) and mixed conditions (daily mean
330 CI $\leqslant$ 1.0) are 0.5, 0.8, and 1.8 °C for the Ngari, Xiao Dongkemadi and Qinghai stations,
331 respectively. However, those for cases based on observed LST are significantly lower with
332 corresponding values of 0.0, -0.1, and 0.2 °C.
333 This indicates that T_{min} estimations based on MODIS LST are greatly affected by clouds. This
334 seems counterintuitive, as it has been shown that T_{min} estimations based on ground observed LST
335 are not significantly affected by clouds (Fig. 6). Thus, the most probable driving factor may be the
336 relatively large amounts of undetected clouds present in MODIS nighttime LST. As daily cloud
337 indexes increase, more undetected cloudy cases may be introduced, thus reducing the accuracy of
338 MODIS nighttime LST (Fig. 4 and Table 2).
339 Figure 8 (upper section) supports this conclusion: under clear conditions, the undetected clouds
340 are rare, and limited accuracy improvements are achieved by removing the few cloudy MODIS

LST records; However, as daily CI constraints ease to 0.5 when cloudy records account for a substantial proportion, obvious improvements appear, and the final accuracies are much closer to and are even better than those based on ground observed LST.

Unlike that of T_{min}, the accuracy variation of T_{max} estimation based on MODIS LST shows trends that are highly consistent with those of cases based on ground observed LST for all of the three sites. As with cases based on ground observed LST, T_{max} estimation based on MODIS LST are found to be greatly affected by clouds. In addition, increases in (T_{max} estimation based on MODIS LST vs. that based on ground observed LST) in accuracy level differences between clear and mixed conditions are much less pronounced compared to those of T_{min}, where difference values are only 0.0, 0.2 and 0.3 °C for the Ngari, Xiao Dongkemadi and Qinghai stations, respectively.

However, the accuracy levels achieved from MODS LST after removing cloudy records are obviously lower than those based on ground observed LST under all cloudiness conditions. This raises questions regarding what this difference in accuracy attribute to? Dominant factors may not be undetected clouds, as was the case for T_{min}. As shown in Fig. 8 (lower section), the removal of cloudy records had somewhat moderate effects on accuracy levels. This may be largely due to much lower erroneous rates of cloud identification for MODIS daytime LST. The obviously lower number of undetected clouds compared to nighttime LST values for the Ngari and Qinghai stations result in relatively limited accuracy improvements. The relatively large decrease in estimation errors for the Xiao Dongkemadi station is mainly due to unexpected higher amounts of undetected clouds in MODIS daytime LST for that site (Table 2 and Fig. 8).

Furthermore, even under clear conditions, the accuracy of T_{max} estimations based on MODIS LST is remarkably lower than that based on ground observed LST (Fig. 7). Thus, the decrease in accuracy levels relative to cases based on ground observed LST may be caused by other factors rather than undetected clouds. This seems odd, especially given that the accuracies of T_{min} estimations based on MODIS LST are very close to or even better than those based on observed LST under clear conditions (Fig. 7).

4.5 Effects of clouds on T_{air} estimation based on MODIS LST and CMA observations

Figure 9 shows the estimation accuracies of T_{air} based on MODIS LST for non-cloudy and cloudy conditions. For the T_{max} estimation, clouds appear to have moderate effects on estimation

accuracies, where 88% of the 92 stations obtained lower RMSEs based on samples from "non-cloudy" conditions relative to cloudy cases. RMSE values are reduced by an average of 0.54 °C. In contrast, effects of clouds on T_{min} estimations are much more significant: the RMSEs of 98% stations are reduced by an average of 1.44 °C. Though hourly observations in the data for CMA stations are lacking, the results for the cloud tests are highly consistent with those based on half-hourly AWS observations.

Furthermore, a comparison between the T_{max} and T_{min} estimation results based on MODIS LST and CMA observations shows that under cloudy conditions, T_{max} estimations (the mean RMSE is 4.3 °C) achieve generally higher levels of accuracy than T_{min} estimations (the mean RMSE is 4.6 °C), whereas non-cloudy conditions produce the opposite effect (3.7 vs. 3.2 °C) illustrating potentially stronger negative effect of cloud on T_{max} estimation than T_{min} .

5 Discussion

5.1 Differences in the effects of clouds on T_{min} and T_{max} estimations based on MODIS LST

From MODIS LST and daily CMA observations, different cloud effects between T_{max} and T_{min} estimations can be identified from Fig. 9. Under cloudy conditions, the existence of more undetected cloudy records in MODIS nighttime LST largely degrades the LST accuracy and results in obviously lower T_{min} estimation accuracy levels. However, why the T_{min} estimations clearly outperform T_{max} under clear conditions (non-cloudy day condition) when both are free of cloud effects remains unknown. One may argue that the so-called "clear" conditions are based on only four satellite instantaneous observations and that actual cloudiness conditions may still be cloudy. Although this is true, our study shows that even under clear conditions, the accuracy of T_{max} estimations based on daytime MODIS LST is much lower than those based on observed LST, whereas the T_{min} estimation based on nighttime MODIS LST shows comparable or even superior accuracy.

From our previous analysis, we can attribute this difference in estimation accuracy between T_{min} and T_{max} to differences between daytime and nighttime MODIS LST. Much lower levels of MODIS daytime LST accuracy than those for nighttime have been found in previous studies (Yu and Ma, 2011; Krishnan et al., 2015; Min et al., 2015), and the validation tests shown in Figures 4 and 5 also supports this conclusions. This precision bias is most likely attributable scale issues

(Wan et al., 2002; Wan, 2008). Single point measurements are difficult to make representative of the 1-km MODIS pixel when ground surfaces are complex (Hall et al., 2008; Coll et al., 2009). Many studies have shown that MODIS daytime LST presents obviously lower levels of validation accuracy than nighttime LST due to high levels of daytime LST heterogeneity (Wang et al., 2008; Coll et al., 2009). In the daytime, cloud and hill shadows within pixels can produce considerable LST heterogeneities while at night, the ground surface becomes cool and more homogeneous when free of solar heating uncertainties (Wang et al., 2008). Oyler et al. (2016) also show that daytime LST exhibits more spatial variation than T_{air} while nighttime LST follows similar spatial patterns as T_{air} as demonstrated in his study.

In addition, it should be noted that clouds also have substantial effects on T_{max} estimation. Thus, it can be concluded that the frequently reported lower estimation accuracies of T_{max} based on MODIS daytime LST compared to those of T_{min} based on nighttime LST (Zhang et al., 2011; Benali et al., 2012; Zhu et al., 2013; Oyler et al., 2016) are mainly due to the mixed effects of the relatively low daytime LST accuracies and clouds.

To further prove this, four CMA stations (Fig. 10) presenting the largest reduction in RMSE values after imposing clear conditions are selected for our T_{min} and T_{max} estimations. They can represent practical application conditions where only daily meteorological observations can be obtained.

For T_{max} estimation (Fig. 11), it is evident that forcing clear conditions has somewhat limited effects on estimation performance. The samples collected under “cloudy day” conditions include outliers far from the fit line derived using samples under “non-cloudy day” conditions. However, the “non-cloudy day” samples still appear rather dispersed with many samples positioned far from the fit line, and especially in the case of stations 89 and 41. This may illustrate mixed effects of both clouds and LST accuracies to some degree.

In contrast, the results of the T_{min} estimation are somewhat inspiring. As shown in Fig. 12, a number of cold-biased outliers that may be undetected cloudy records are captured by employing cloudy conditions. More importantly, the “non-cloudy day” condition samples achieve a much better fit. This not only demonstrates that undetected cloudy records are ubiquitous in MODIS nighttime LST and that amounts can often be quite large but also that the influence of clouds on T_{min} estimations with true LST (i.e., without undetected clouds) is not substantial. Though the actual cloudiness conditions are rather unpredictable and quite a few “good” samples around the

"non-cloudy day" fit line are also included in the "cloudy day" group, we consider constraining all four MODIS observations for each day as non-cloudy as an efficient way to build a good fit among T_{min} estimations using MODIS nighttime LST as long as the amount of valid samples is sufficient. This method can benefit studies requiring accurate T_{min} estimations based on remotely sensed LST.

5.2 Uncertainty and error sources

Emissivity issues may have caused the observed LST computation errors. Constant emissivity values for the Ngari and Qinghai stations are used in our study, although this may not be reasonable for non-growing seasons. However, the sensitivity experiments show that the influence of emissivity values is not significant.

The $\leq$ 15 min discrepancy may introduce uncertainties in data that intersect T_{air}, MODIS and observed LST. Its influence is considered to be insignificant. Nighttime LST changes gently and half-hourly observations can be used for MODIS LST validation as indicated in Wang et al. (2008). T_{air} also respond relatively slowly to LST, and MODIS daytime LST shows a strong relationship to T_{air} at a similar time discrepancy level ($\leq$ 12 min) to that shown by Williamson et al. (2013). Spatial heterogeneities within MODIS pixels of AWS may pose problems. As shown in Fig. 1, such problems may not be severe, as land cover within the pixels of the three AWSs appears to be largely homogeneous. The data quality of MODIS LST does not receive sufficient consideration in this study. MODIS LST production involves the use of internal data quality flags, and previous studies demonstrate that data quality is related to cloud contamination (Williamson et al., 2013; Østby et al., 2014).

The validation accuracy of MODIS LST is affected by data quality (Krishnan et al., 2015). However, rigid data quality constraints may severely decrease sample sizes due to relatively short observation periods (1−2 years) used. This study presents results of general quality status, and extreme low quality data (QC = 3) have been removed. Other factors including wind speeds and sensor view zenith angles may affect results related to MODIS LST validation and the relationship between T_{air} and LST. According to Wang et al. (2008), the validation results are not or are weakly affected by wind speed and the sensor view zenith angle. Wind speed has a limited effect on the T_{air}-LST relationship, as shown by Gallo et al. (2011).

In addition, the results shown here are highly consistent across the three AWSs dominated by three types of land cover, thus indicating that our results may be highly representative and that other factors may not have played a key role.

6 Conclusion

Cloud effects on T_{min} and T_{max} estimations according to MODIS LST are analyzed based on detailed ground based observations from three valuable AWSs and based on data from 92 CMA stations over the TP. Cloudiness is quantified using an efficient method based on ground measurements of air temperature and downwelling longwave radiation. Comparisons made between in-situ cloudiness observations and MODIS claimed clear-sky records shows that erroneous rates of MODIS nighttime cloud detection are obviously larger than those for the daytime. Our MODIS LST validation for different cloudiness constraining conditions reveals that the accuracy of MODIS nighttime LST is severely affected by undetected clouds. However, the accuracies of MODIS daytime LST do not seem to be influenced considerably by undetected clouds.

Cloud effect tests show that T_{min} estimations based on MODIS LST are mainly affected by large errors introduced by undetected clouds in nighttime LST. However, clouds mainly influence T_{max} estimation by affecting the relationship between T_{max} and daytime LST. The effects of undetected clouds in daytime LST are relatively weak. Frequently reported larger errors in T_{max} estimations based on daytime LST than those of T_{min} based on nighttime LST may be largely attributed to relatively large errors of MODIS daytime LST resulting from scale issues. Tests based on CMA station observations further validate our results and show that constraining all four MODIS observations per day as non-cloudy helps rule out undetected cloudy records while building good T_{min} estimation fit.

This study presents useful findings on the key effects of clouds on T_{air} estimation based on MODIS LST that can alleviate problems of severe data sparseness over the TP. More efficient cloud detection methods for MODIS nighttime LST are needed for T_{min} estimations. T_{max} estimation based on daytime LST is rather challenging due to the complex effects of daily cloudiness conditions in combination with scale issues.

Author Contribution

Professor Tian, He and Tang observed and provided the data of stations Nagri, Xiao Dongkemadi and Qinghai, respectively. Professor Fan Zhang and Associate Professor Guoqing Zhang gave many valuable suggestions to improve the manuscript. Dr. Hongbo Zhang designed the experiments and wrote the manuscript.

Acknowledgment

This work was supported by the Chinese Academy of Sciences "Strategic Priority Research Program (B)" (Grant No. XDB03030300); and by the National Natural Science Foundation of China (Grant No. 41422101, 41271079, 41130638). We thank the Tanggula Station for Cryosphere Environment Observation and Research and the Ngari Station for Desert Environment Observation and Research for providing ground measurements of longwave radiation and air temperature data. The Qinghai station data were downloaded from AsiaFlux (www.asiaflux.net). We would like to thank Dr. Yanhong Tang for providing the ground measurements for the Qinghai station. We are grateful to the Chinese Meteorology Administration for providing air temperature data.

References

Ackerman, S. A., Strabala, K. I., Menzel, W. P., Frey, R. A., Moeller, C. C., and Gumley, L. E.: Discriminating clear sky from clouds with MODIS, J. Geophys. Res.-Atmos., 103, 32141-32157, 10.1029/1998jd200032, 1998.

Ackerman, S. A., Holz, R. E., Frey, R., Eloranta, E. W., Maddux, B. C., and McGill, M.: Cloud Detection with MODIS. Part II: Validation, Journal of Atmospheric and Oceanic Technology, 25, 1073-1086, 10.1175/2007JTECHA1053.1, 2008.

Benali, A., Carvalho, A. C., Nunes, J. P., Carvalhais, N., and Santos, A.: Estimating air surface temperature in Portugal using MODIS LST data, Remote Sensing of Environment, 124, 108-121, 10.1016/j.rse.2012.04.024, 2012.

Coll, C., Wan, Z., and Galve, J. M.: Temperature - based and radiance - based validations of the V5 MODIS land surface temperature product, Journal of Geophysical Research: Atmospheres, 114, 2009.

Dai, A., Trenberth, K. E., and Karl, T. R.: Effects of clouds, soil moisture, precipitation, and water vapor on diurnal temperature range, Journal of Climate, 12, 2451-2473, 10.1175/1520-0442(1999)012<2451:eocsmp>2.0.co;2, 1999.

Emamifar, S., Rahimikhoob, A., and Noroozi, A. A.: Daily mean air temperature estimation from MODIS

land surface temperature products based on M5 model tree, International Journal of Climatology, 33, 3174-3181, 10.1002/joc.3655, 2013.

Fu, G., Shen, Z., Zhang, X., Shi, P., Zhang, Y., and Wu, J.: Estimating air temperature of an alpine meadow on the Northern Tibetan Plateau using MODIS land surface temperature, Acta Ecologica Sinica, 31, 8-13, 10.1016/j.chnaes.2010.11.002, 2011.

Gallo, K., Hale, R., Tarpley, D., and Yu, Y.: Evaluation of the relationship between air and land surface temperature under clear-and cloudy-sky conditions, Journal of Applied Meteorology and Climatology, 50, 767-775, 2011.

Giesen, R., Van den Broeke, M., Oerlemans, J., and Andreassen, L.: Surface energy balance in the ablation zone of Midtdalsbreen, a glacier in southern Norway: interannual variability and the effect of clouds, Journal of Geophysical Research: Atmospheres, 113, 2008.

Good, E.: Daily minimum and maximum surface air temperatures from geostationary satellite data, Journal of Geophysical Research: Atmospheres, 120, 2306-2324, 10.1002/2014JD022438, 2015.

Hall, D. K., Box, J. E., Casey, K. A., Hook, S. J., Shuman, C. A., and Steffen, K.: Comparison of satellite-derived and in-situ observations of ice and snow surface temperatures over Greenland, Remote Sensing of Environment, 112, 3739-3749, 2008.

Huang, J., Wang, T., Wang, W., Li, Z., and Yan, H.: Climate effects of dust aerosols over East Asian arid and semiarid regions, Journal of Geophysical Research: Atmospheres, 119, 11,398-311,416, 10.1002/2014JD021796, 2014.

Huintjes, E., Sauter, T., Schröter, B., Maussion, F., Yang, W., Kropácek, J., Buchroithner, M., Scherer, D., Kang, S., and Schneider, C.: Evaluation of a coupled snow and energy balance model for Zhadang glacier, Tibetan Plateau, using glaciological measurements and time-lapse photography, Arctic, Antarctic, and Alpine Research, 47, 573-590, 2015.

Jang, J.-D., Viau, A., and Anctil, F.: Neural network estimation of air temperatures from AVHRR data, International Journal of Remote Sensing, 25, 4541-4554, 2004.

Kilibarda, M., Hengl, T., Heuvelink, G. B. M., Gräler, B., Pebesma, E., Perčec Tadić, M., and Bajat, B.: Spatio-temporal interpolation of daily temperatures for global land areas at 1 km resolution, Journal of Geophysical Research: Atmospheres, 119, 2294-2313, 10.1002/2013JD020803, 2014.

Krishnan, P., Kochendorfer, J., Dumas, E. J., Guillevic, P. C., Baker, C. B., Meyers, T. P., and Martos, B.: Comparison of in-situ, aircraft, and satellite land surface temperature measurements over a NOAA Climate Reference Network site, Remote Sensing of Environment, 165, 249-264, 2015.

Langer, M., Westermann, S., and Boike, J.: Spatial and temporal variations of summer surface temperatures of wet polygonal tundra in Siberia - implications for MODIS LST based permafrost monitoring, Remote Sensing of Environment, 114, 2059-2069, 10.1016/j.rse.2010.04.012, 2010.

Lin, S. P., Moore, N. J., Messina, J. P., DeVisser, M. H., and Wu, J. P.: Evaluation of estimating daily maximum and minimum air temperature with MODIS data in east Africa, Int. J. Appl. Earth Obs. Geoinf., 18, 128-140, 10.1016/j.jag.2012.01.004, 2012.

Lin, X., Pielke Sr, R. A., Mahmood, R., Fiebrich, C. A., and Aiken, R.: Observational evidence of temperature trends at two levels in the surface layer, Atmos. Chem. Phys., 16, 827-841, 10.5194/acp-16-827-2016, 2016.

Min, W., Yueqing, L. I., and Zhou, J.: Validation of MODIS Land Surface Temperature Products in East of the Qinghai-Xizang Plateau, Plateau Meteorology, 2015.

Østby, T. I., Schuler, T. V., and Westermann, S.: Severe cloud contamination of MODIS Land Surface Temperatures over an Arctic ice cap, Svalbard, Remote Sensing of Environment, 142, 95-102,

10.1016/j.rse.2013.11.005, 2014.
Oyler, J. W., Ballantyne, A., Jencso, K., Sweet, M., and Running, S. W.: Creating a topoclimatic daily air temperature dataset for the conterminous United States using homogenized station data and remotely sensed land skin temperature, International Journal of Climatology, 35, 2258-2279, 2015.
Oyler, J. W., Dobrowski, S. Z., Holden, Z. A., and Running, S. W.: Remotely Sensed Land Skin Temperature as a Spatial Predictor of Air Temperature across the Conterminous United States, Journal of Applied Meteorology and Climatology, 2016.
Parmentier, B., McGill, B. J., Wilson, A. M., Regetz, J., Jetz, W., Guralnick, R., Tuanmu, M. N., and Schildhauer, M.: Using multi‐timescale methods and satellite‐derived land surface temperature for the interpolation of daily maximum air temperature in Oregon, International Journal of Climatology, 35, 3862-3878, 2015.
Platnick, S., King, M. D., Ackerman, S. A., Menzel, W. P., Baum, B. A., Riedi, J. C., and Frey, R. A.: The MODIS cloud products: algorithms and examples from Terra, IEEE Trans. Geosci. Remote Sensing, 41, 459-473, 10.1109/TGRS.2002.808301, 2003.
Shamir, E., and Georgakakos, K. P.: MODIS Land Surface Temperature as an index of surface air temperature for operational snowpack estimation, Remote Sensing of Environment, 152, 83-98, 2014.
Shen, S. H., and Leptoukh, G. G.: Estimation of surface air temperature over central and eastern Eurasia from MODIS land surface temperature, Environ. Res. Lett., 6, 8, 10.1088/1748-9326/6/4/045206, 2011.
Van Den Broeke, M., Reijmer, C., Van As, D., and Boot, W.: Daily cycle of the surface energy balance in Antarctica and the influence of clouds, International Journal of Climatology, 26, 1587-1605, 10.1002/joc.1323, 2006.
Vancutsem, C., Ceccato, P., Dinku, T., and Connor, S. J.: Evaluation of MODIS land surface temperature data to estimate air temperature in different ecosystems over Africa, Remote Sensing of Environment, 114, 449-465, 10.1016/j.rse.2009.10.002, 2010.
Wan, Z., and Dozier, J.: A generalized split-window algorithm for retrieving land-surface temperature from space, Geoscience and Remote Sensing, IEEE Transactions on, 34, 892-905, 1996.
Wan, Z., Zhang, Y., Zhang, Q., and Li, Z.-l.: Validation of the land-surface temperature products retrieved from Terra Moderate Resolution Imaging Spectroradiometer data, Remote sensing of Environment, 83, 163-180, 2002.
Wan, Z.: New refinements and validation of the MODIS Land-Surface Temperature/Emissivity products, Remote Sensing of Environment, 112, 59-74, 10.1016/j.rse.2006.06.026, 2008.
Wang, W., Liang, S., and Meyers, T.: Validating MODIS land surface temperature products using long-term nighttime ground measurements, Remote Sensing of Environment, 112, 623-635, 2008.
Westermann, S., Langer, M., and Boike, J.: Spatial and temporal variations of summer surface temperatures of high-arctic tundra on Svalbard - Implications for MODIS LST based permafrost monitoring, Remote Sensing of Environment, 115, 908-922, 10.1016/j.rse.2010.11.018, 2011.
Westermann, S., Langer, M., and Boike, J.: Systematic bias of average winter-time land surface temperatures inferred from MODIS at a site on Svalbard, Norway, Remote Sensing of Environment, 118, 162-167, 2012.
Williamson, S. N., Hik, D. S., Gamon, J. A., Kavanaugh, J. L., and Koh, S.: Evaluating cloud contamination in clear-sky MODIS Terra daytime land surface temperatures using ground-based meteorology station observations, Journal of Climate, 26, 1551-1560, 2013.

Wu, Y., Wang, N., He, J., and Jiang, X.: Estimating mountain glacier surface temperatures from Landsat-ETM+ thermal infrared data: A case study of Qiyi glacier, China, Remote Sensing of Environment, 163, 286-295, 2015.

Xu, Y., Knudby, A., and Ho, H. C.: Estimating daily maximum air temperature from MODIS in British Columbia, Canada, International Journal of Remote Sensing, 35, 8108-8121, 10.1080/01431161.2014.978957, 2014.

Yang, W., Guo, X., Yao, T., Yang, K., Zhao, L., Li, S., and Zhu, M.: Summertime surface energy budget and ablation modeling in the ablation zone of a maritime Tibetan glacier, Journal of Geophysical Research: Atmospheres, 116, 2011.

Yu, J., Zhang, G., Yao, T., Xie, H., Zhang, H., Ke, C., and Yao, R.: Developing Daily Cloud-Free Snow Composite Products From MODIS Terra–Aqua and IMS for the Tibetan Plateau, IEEE Trans. Geosci. Remote Sensing, 54, 2171-2180, 10.1109/TGRS.2015.2496950, 2016.

Yu, W., and Ma, M.: Validation of the MODIS Land Surface Temperature Products——A Case Study of the Heihe River Basin, Remote Sensing Technology & Application, 26, 705-712, 2011.

Zeng, L., Wardlow, B. D., Tadesse, T., Shan, J., Hayes, M. J., Li, D., and Xiang, D.: Estimation of daily air temperature based on MODIS land surface temperature products over the corn belt in the US, Remote Sens., 7, 951-970, 2015.

Zhang, H., Zhang, F., Ye, M., Che, T., and Zhang, G.: Estimating daily air temperatures over the Tibetan Plateau by dynamically integrating MODIS LST data, Journal of Geophysical Research: Atmospheres, 10.1002/2016JD025154, 2016. (*in press*)

Zhang, W., Huang, Y., Yu, Y. Q., and Sun, W. J.: Empirical models for estimating daily maximum, minimum and mean air temperatures with MODIS land surface temperatures, International Journal of Remote Sensing, 32, 9415-9440, 10.1080/01431161.2011.560622, 2011.

Zhu, W., Lű, A., and Jia, S.: Estimation of daily maximum and minimum air temperature using MODIS land surface temperature products, Remote Sensing of Environment, 130, 62-73, 10.1016/j.rse.2012.10.034, 2013.

643 Table 1. Summary of the AWS sites

644

AWS	Lon/Lat	Mean annual Precipitation (mm)	Mean annual air temperature (°C)	Elevation (m)	Land cover	Time period
Xiao Dongkemadi	92.08/33.07	680	-8.6	5621	Glacier	2009.1 − 2009.12
Ngari	79.70/33.39	125	1.2	4270	Desert grassland	2012.6 − 2013.12
Qinghai	101.30/37.60	567	-1.7	3250	Alpine meadow	2003.1 − 2004.12

645

646 Table 2. Undetected MODIS LST clouds at 3 AWSs

647

Site	Ratio of undetected cloudy records			
	Terra day (%)	Terra night (%)	Aqua day (%)	Aqua night (%)
Ngari	5	3	3	15
Xiao Dongkemadi	12	15	11	37
Qinghai	3	20	3	50
Average	7	13	6	34

648

649

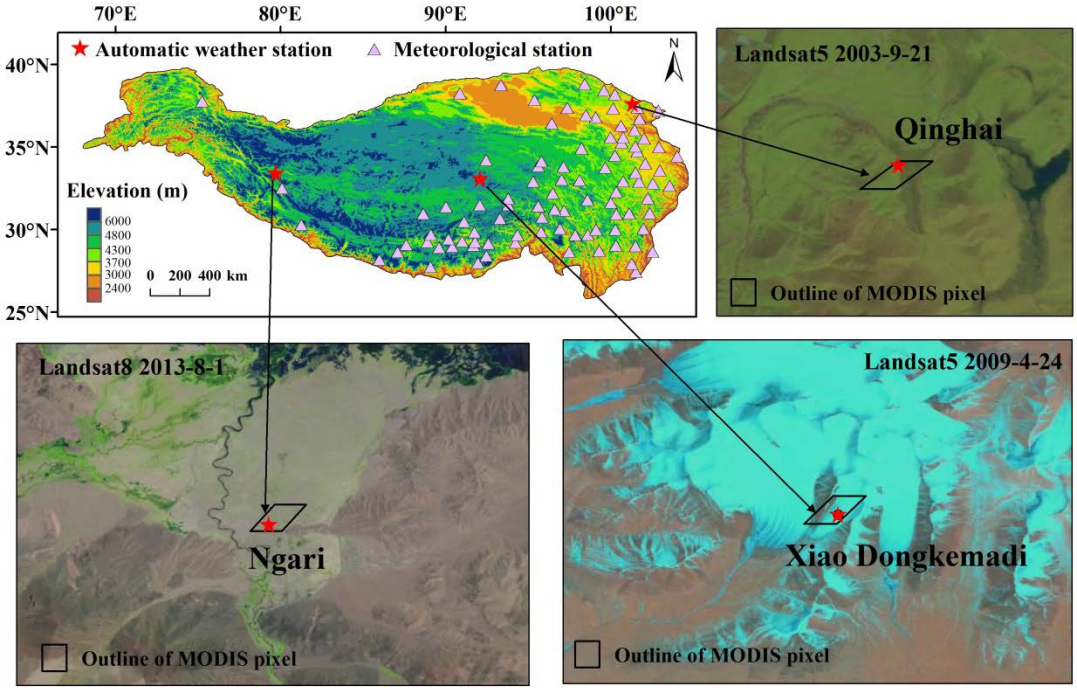

650

651

652 Figure 1: Map of the TP marking AWS and meteorological station locations. Landsat images

653 observed during the time period for data used in this study are also shown in natural color modes

654 with acquired dates. The outline of the MODIS grid is also plotted.

655

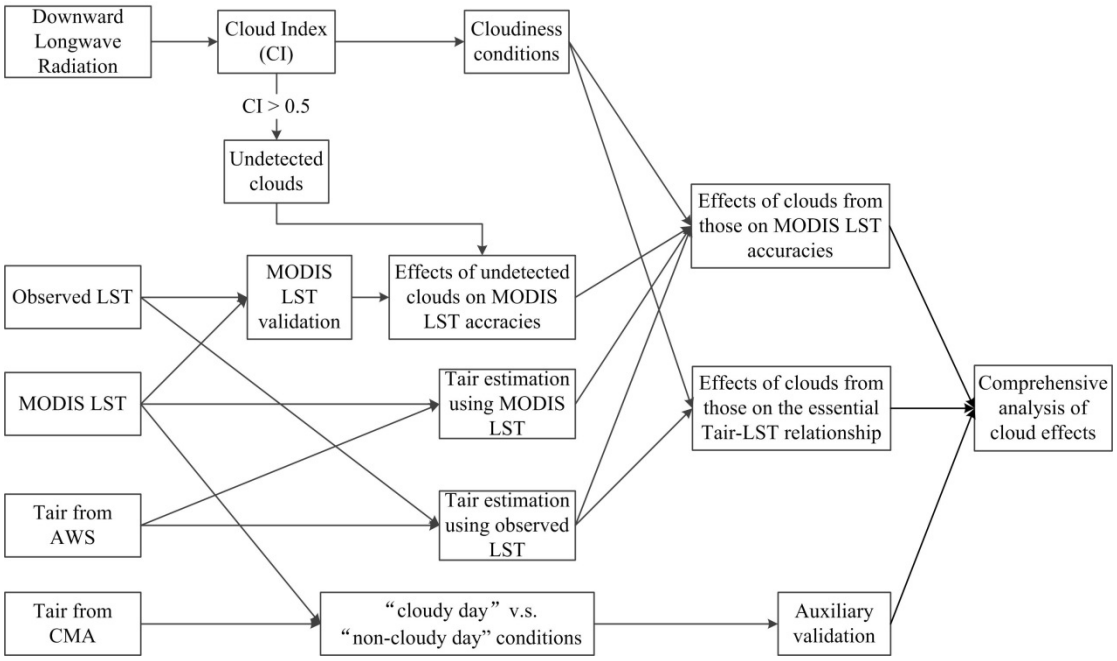

Figure 2: The flow chart describing the analysis and validation of cloud effects on air temperature estimation using MODIS LST in this study.

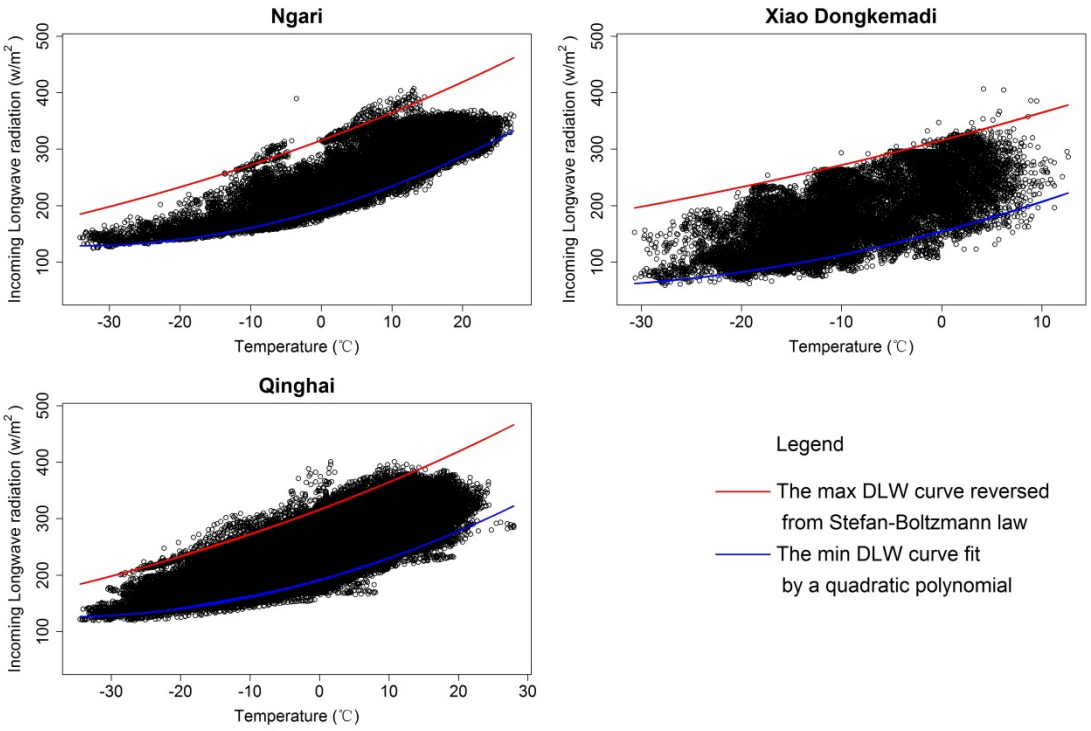

Figure 3: The distribution of observed downward longwave radiation (DLW) under different air temperatures. The red line represents the max DLW curve reversed from the Stefan-Boltzmann law. The blue line is the min DLW curve fitted by a quadratic polynomial.

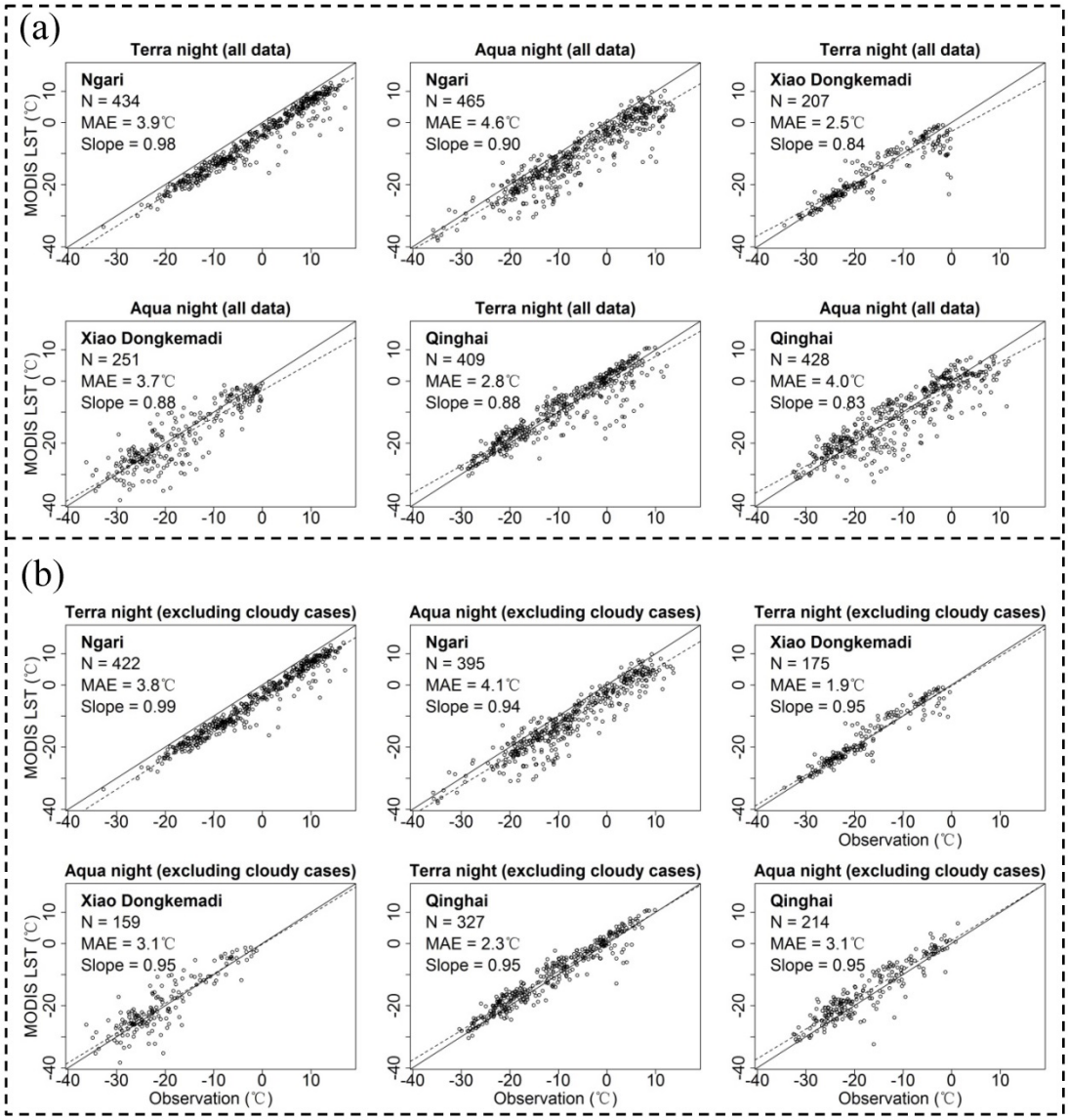

Figure 4: Validation of MODIS nighttime LST before (a) and after (b), excluding cloudy cases.

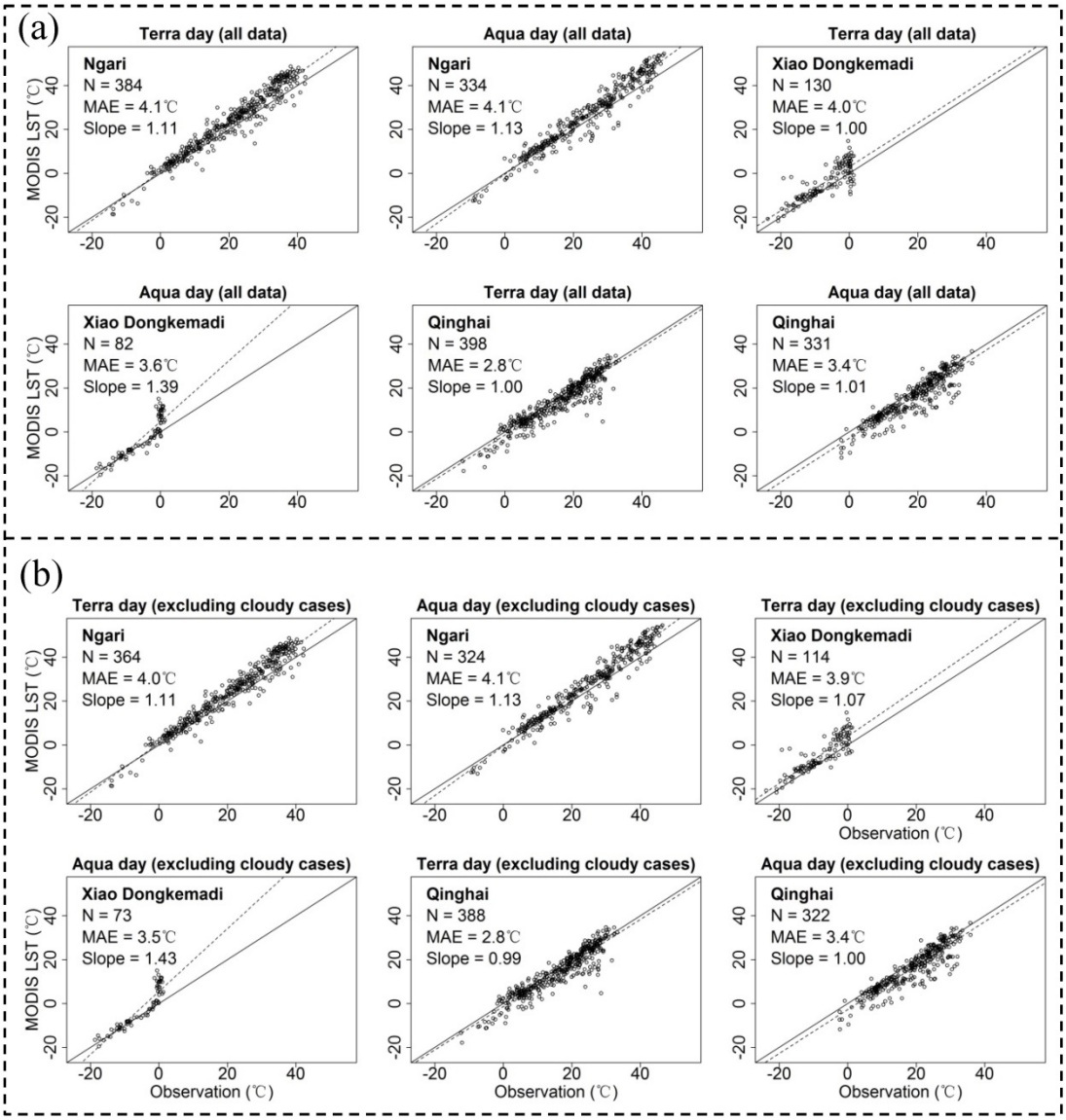

Figure 5: Validation of MODIS daytime LST before (a) and after (b), excluding cloudy cases.

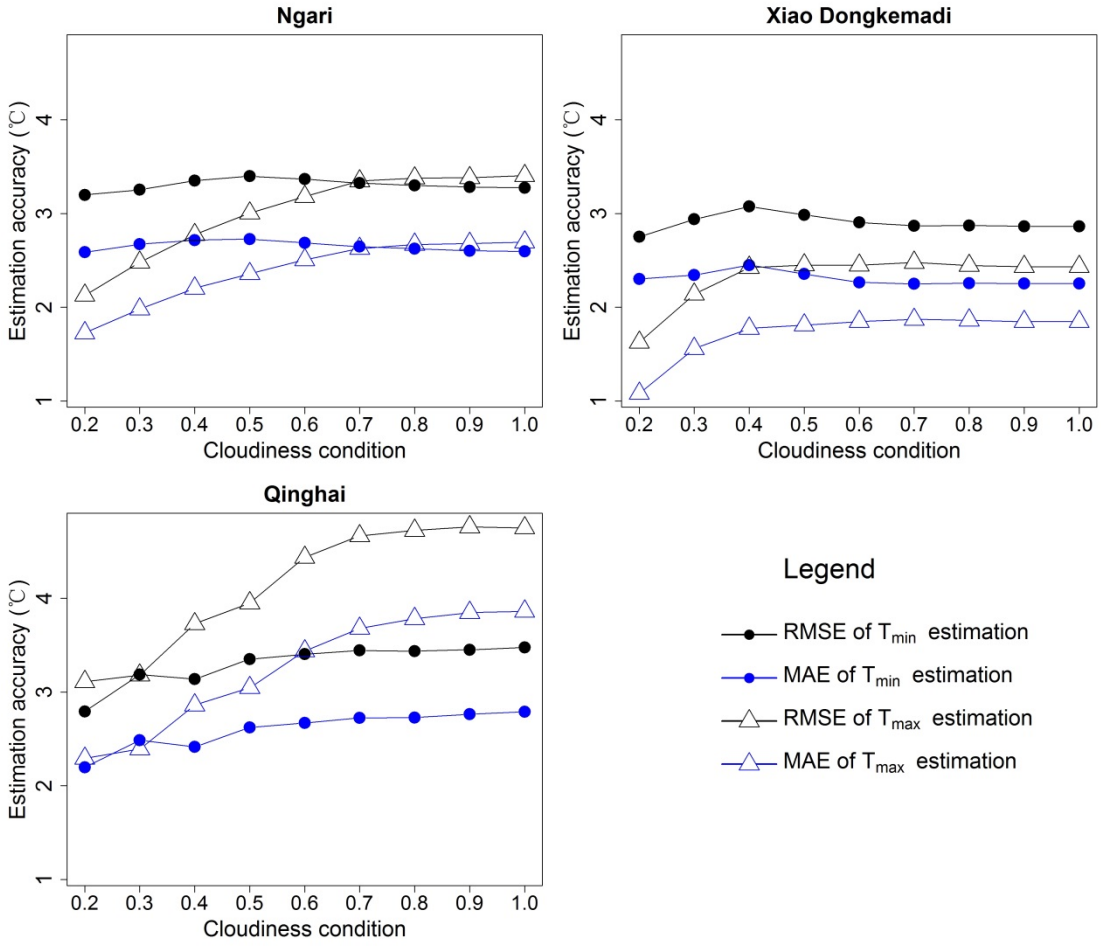

Figure 6: Accuracies (RMSE and MAE) of T_{max} and T_{min} estimations based on ground measured LST under different cloudiness conditions across the three sites. The "cloudiness condition" is the constraining condition of the daily averaged cloudiness index (CI). For example, a cloudiness condition of 0.2 denotes a constraining daily mean of CI ≤ 0.2.

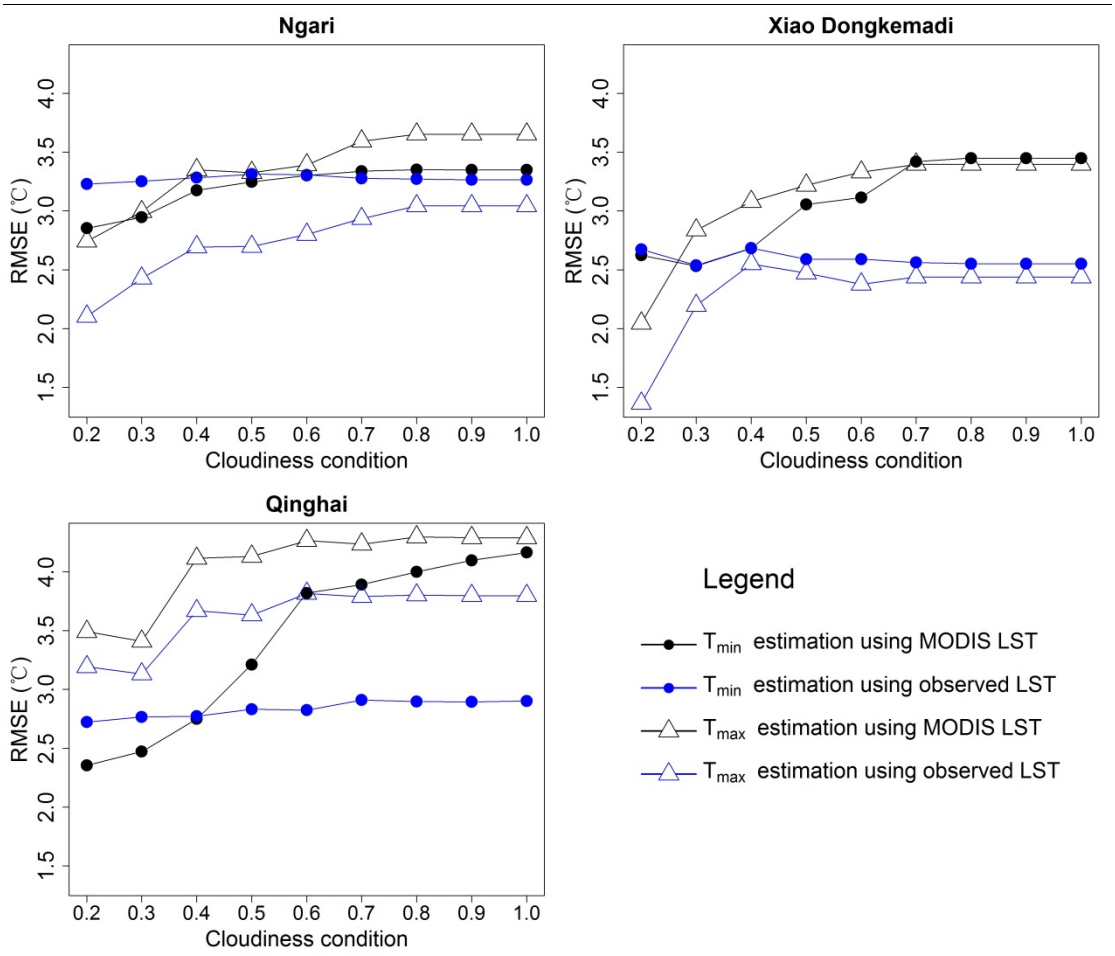

Figure 7: Accuracies (RMSE) of T_{max} and T_{min} estimations based on ground measured or MODIS LST under different cloudiness conditions for the three AWSs. The "cloudiness condition" is the constraining condition of the daily averaged cloudiness index (CI). For example, a cloudiness condition of 0.2 denotes a constraining daily mean of $CI \leq 0.2$.

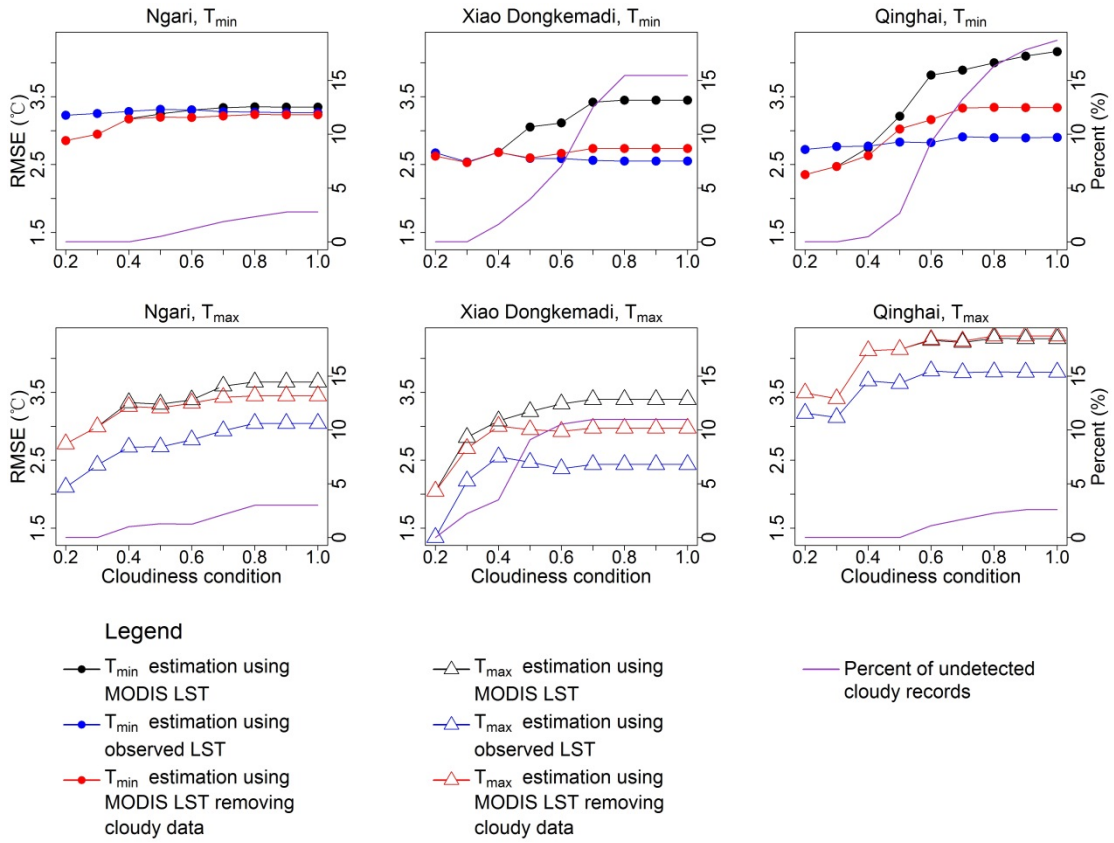

692

693 Figure 8: Comparisons between T_{min} and T_{max} estimation accuracies based on MODIS LST,

694 MODIS LST without cloudy data, and observed LST under different cloudiness conditions for the

695 three AWSs.

696

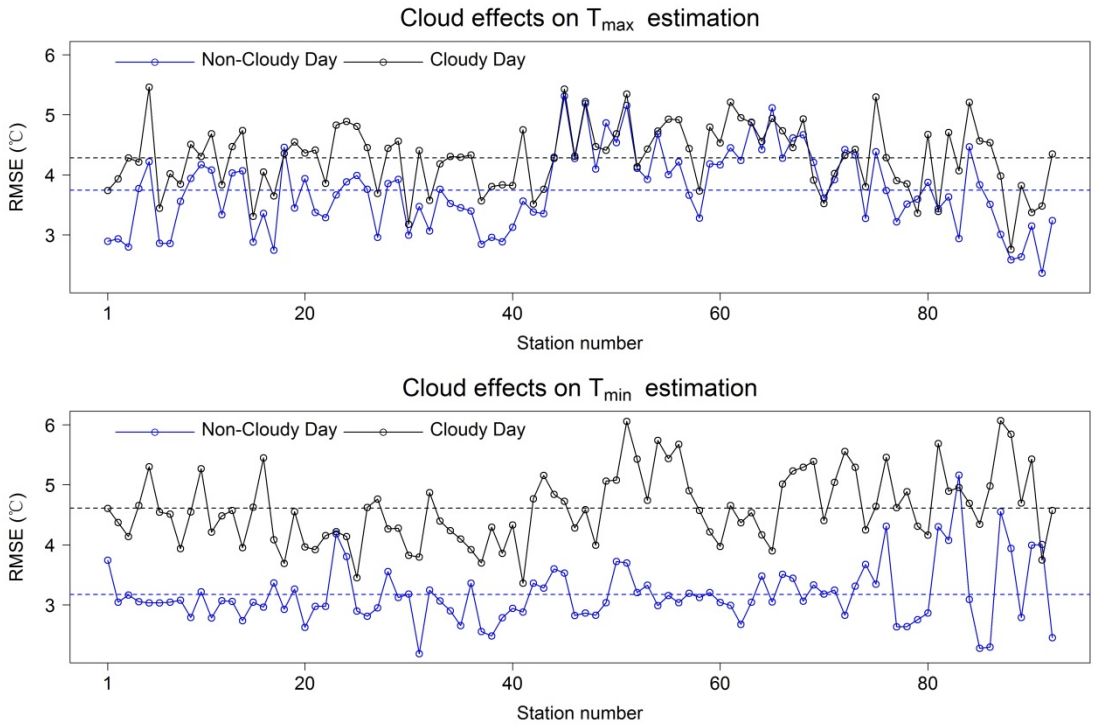

Figure 9: Comparisons of T_{air} estimation accuracy levels based on MODIS LST and CMA observations for “non-cloudy day” and “cloudy day” conditions.

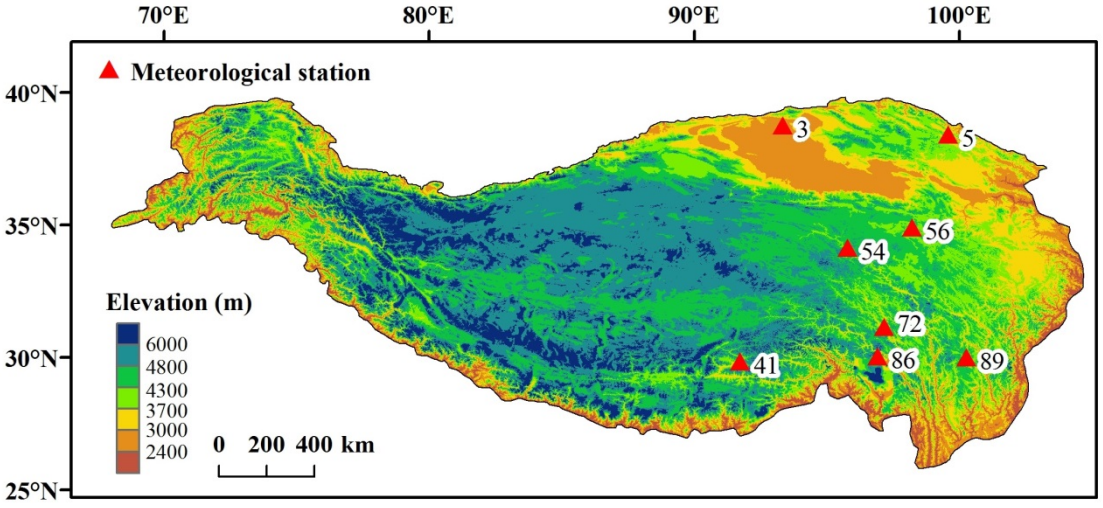

Figure 10: Locations of 4 representative CMA stations for T_{min} (NO. 54, 56, 72, 86) and T_{max} (NO. 3, 5, 41, 89) estimations.

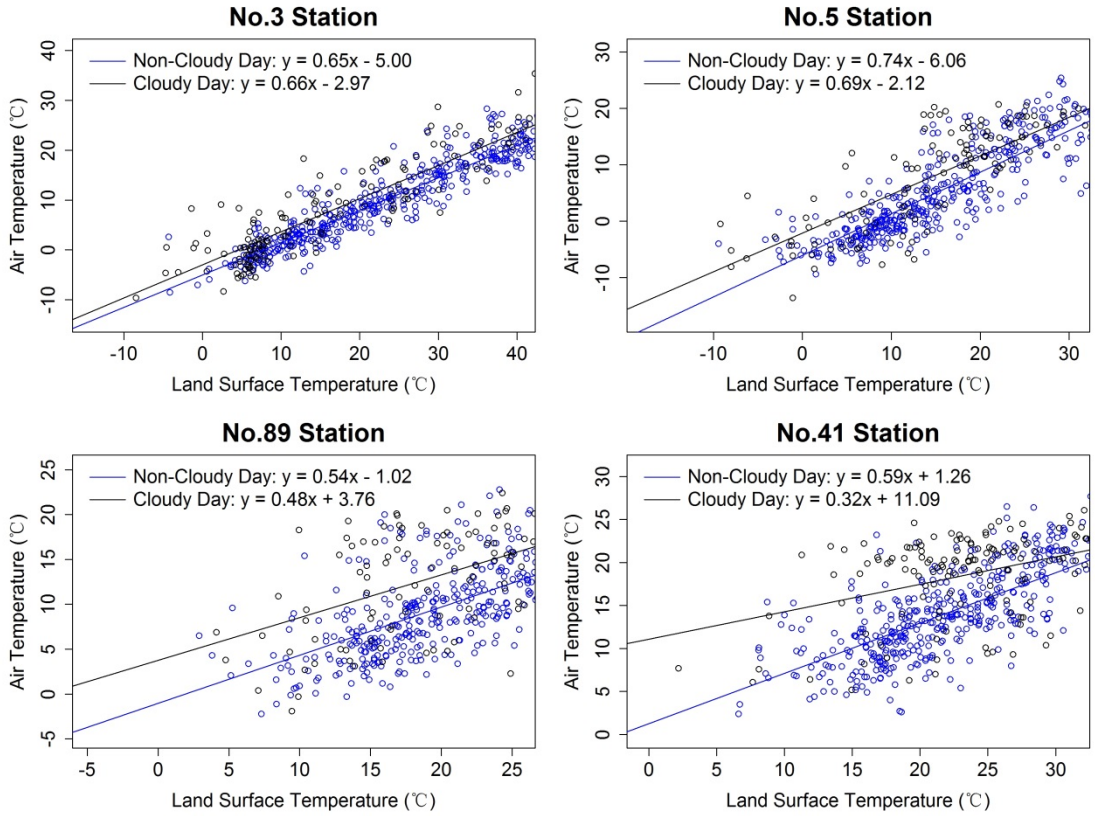

Figure 11: Comparisons of T_{max} estimation accuracy between “cloudy day” and “non-cloudy day” conditions at four meteorological stations presenting the largest decline in RMSE.

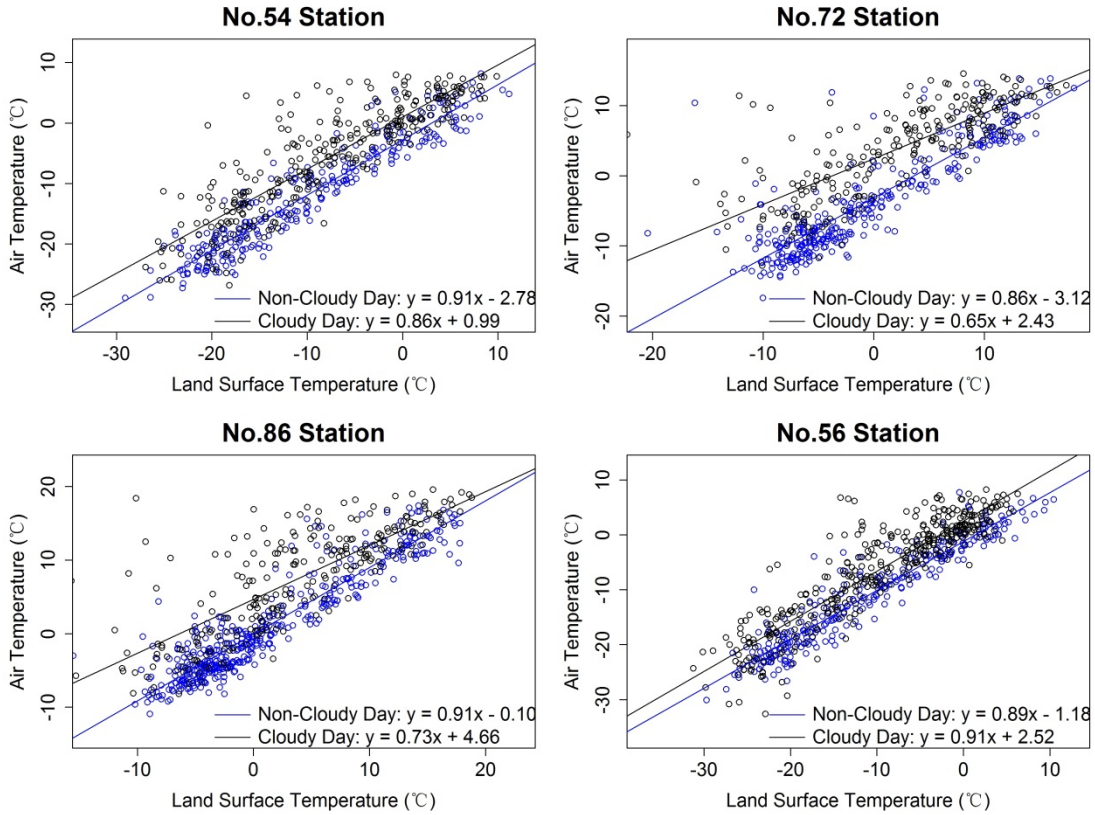

714

715

716 Figure 12: Comparisons of T_{min} estimation accuracy between “cloudy day” and “non-cloudy day”

717 conditions at four meteorological stations presenting the largest decline in RMSE.

718

719

720